



OPEN ACCESS

EDITED BY

Tao Li,
South China Sea Institute of
Oceanology, Chinese Academy of
Sciences, China

REVIEWED BY

Alexei E. Solovchenko,
Lomonosov Moscow State
University, Russia
Hongli Cui,
Shanxi Agricultural University, China
Shuhei Ota,
National Institute for Environmental
Studies (NIES), Japan

*CORRESPONDENCE

Guozhen Liu
gzhliu@hebau.edu.cn
Ming Yang
shmym@hebau.edu.cn

SPECIALTY SECTION

This article was submitted to
Marine Biotechnology and
Bioproducts,
a section of the journal
Frontiers in Marine Science

RECEIVED 05 July 2022

ACCEPTED 02 August 2022

PUBLISHED 23 August 2022

CITATION

Xu H, Yang J, Wang X, Peng Q, Han Y,
Liu X, Liu K, Dou S, Li L, Liu G and
Yang M (2022) Starch accumulation
dynamics and transcriptome analysis
of *Chlorella sorokiniana* during
transition of sulfur nutritional status.
Front. Mar. Sci. 9:986400.
doi: 10.3389/fmars.2022.986400

COPYRIGHT

© 2022 Xu, Yang, Wang, Peng, Han, Liu,
Liu, Dou, Li, Liu and Yang. This is an
open-access article distributed under
the terms of the [Creative Commons
Attribution License \(CC BY\)](https://creativecommons.org/licenses/by/4.0/). The use,
distribution or reproduction in other
forums is permitted, provided the
original author(s) and the copyright
owner(s) are credited and that the
original publication in this journal is
cited, in accordance with accepted
academic practice. No use,
distribution or reproduction is
permitted which does not comply with
these terms.

Starch accumulation dynamics and transcriptome analysis of *Chlorella sorokiniana* during transition of sulfur nutritional status

Haiqing Xu¹, Jinzhi Yang¹, Xu Wang¹, Qing Peng¹,
Yanxia Han¹, Xudong Liu¹, Kexin Liu¹, Shijuan Dou^{1,2},
Liyun Li^{1,2}, Guozhen Liu^{1,2,3*} and Ming Yang^{1,2,3*}

¹College of Life Sciences, Hebei Agricultural University, Baoding, China, ²Hebei Key Laboratory of Plant Physiology and Molecular Pathology, Baoding, China, ³Hebei Engineering Research Center for Agricultural Waste Resource Utilization, Baoding, China

Microalgae can effectively accumulate starch by using nutritional limitation methods in the context of bioalcohol fuel production. However, relatively few studies have focused on starch accumulation in microalgae and its molecular basis, especially under sulfur limitation conditions. In this study, the starch accumulation dynamics and physiological responses of *Chlorella sorokiniana* under sulfur starvation (SS) and sulfur replenishment (SR) conditions were investigated, and the genes involved in the transcriptional regulation were explored using RNA-seq. The starch content in *C. sorokiniana* cells significantly increased from 1.6% to 55.0% of dry weight within 24 h under SS conditions, and then, it decreased to 3.4% within 12 h after transition to SR conditions. However, cell growth was inhibited, and pigment content decreased under SS conditions. Using RNA-seq analysis, a total of 9720 differentially expressed genes (DEGs) induced by sulfur status were obtained. These genes were narrowed down to 454 starvation and replenishment cross-validated (SRV)-DEGs, among which 283 SRV-DEGs were significantly up-regulated and 171 SRV-DEGs were down-regulated under SS conditions, and returned to their previous state under SR conditions. The SRV-DEGs enriched in the sulfate metabolism pathway were all up-regulated under SS conditions after 6 h to speed up the sulfur metabolic cycle, and the transcriptional abundance of a sulfate transporter (SULTR4), cysteine synthase [O-acetylserine(thiol)-lyase] (OASTL), serine acetyltransferase (SAT), and methanethiol oxidase (SELENBP1) increased 8.6-fold, 12.6-fold, 8.7-fold, and 12.4-fold, respectively. Protein synthesis was correspondingly inhibited, which resulted in the reallocation of carbon and elevated the starch synthesis pathway, in which the expressions of glycogen branching enzyme (GBE) and starch synthase (SS) were up-regulated 12.0- and 3.0-fold, respectively. The fatty acid desaturase (FAD) and phosphatidic acid phosphatase (PAP) in the lipid synthesis pathway were strongly up-regulated 8.8- and 16.2-fold, respectively, indicating the competitive synthesis of lipids. The down-regulation of SRV-DEGs associated

with carbon fixation, such as those in the Calvin cycle, possibly affected cell growth. The time-resolved transcriptional analysis identified the SRV-DEGs, revealing the underlying starch accumulation mechanism, as well as the relationship with cell growth and lipid synthesis.

KEYWORDS

Chlorella sorokiniana, sulfur-starvation, sulfur-replenishment, transcriptomic dynamics, starch metabolism

Introduction

Microalgae have been recognized as a potential feedstock for biofuel production, because they can efficiently capture CO₂ via photosynthesis and can be continuously cultivated, regardless of the season or climate (Chen et al., 2013; Su et al., 2017). Microalgae accumulate lipids, primarily triacylglycerides (TAGs), which can be used for biodiesel production. Moreover, in the context of bioalcohol fuel production, microalgae can accumulate carbohydrates in the form of starch and cellulose, which can be used for biofuel fermentation (Chen et al., 2013). Importantly, the biomass conversion of microalgae is more effective than that of lignocellulosic materials because of the absence of lignin and its low hemicellulose content (Demuez et al., 2015).

The carbohydrates in microalgae are derived from photosynthesis and carbon fixation metabolism. It has been reported that the content of starch, which is the main form of carbohydrate, accumulated in microalgae varies with species and is dependent on the different culture conditions (Lakatos et al., 2019). In order to generate microalgae biomass with a high starch content, various studies have focused on (1) adjusting the environmental culture conditions, such as irradiance, temperature variation, pH shift, and CO₂ supplement (Chen et al., 2013); (2) nutrient (nitrogen, phosphorus, and sulfur) limitations (Ran et al., 2019); and (3) metabolic regulation in carbohydrate synthesis and degradation (Wang et al., 2017).

The manipulation of nitrogen, phosphate, and sulfur supplies has been the most effective strategy for improving starch accumulation in several microalgae species, such as *Tetraselmis subcordiformis* (Yao et al., 2012; Yao et al., 2018), *Parachlorella kessleri* (Mizuno et al., 2013), *Chlorella vulgaris* (Fernandes et al., 2013), and *Chlamydomonas reinhardtii* (Gardner et al., 2012), in which the starch content was found to reach 37.0–69.3% of the dry biomass. The sulfur limitation (S-limitation) method seemed to be more effective than both the nitrogen and phosphate limitation methods (Brányiková et al., 2011; Ran et al., 2019). It is generally acknowledged that a lack of nutrients can exert stress on microalgae, leading to changes in

cellular metabolic processes and the accumulation of energy storage metabolites, such as starch and lipids. However, this also causes oxidative stress, which leads to a decline in photosynthetic activity and, consequently, a reduction in the overall production of storage metabolites (Chen et al., 2013). It has been suggested that the tradeoff between microalgal growth and the production of storage metabolites should be carefully considered in order to optimize the nutrient manipulation strategy (Ran et al., 2019).

To further improve the overall starch accumulation for microalgae-based biofuel production, it is important to determine the parameters of the stress-induced accumulation of starch and the growth inhibition of microalgae, and to elucidate the underlying metabolic mechanisms. In recent years, the responses of microalgae, such as *C. reinhardtii*, *Tetraselmis* sp., *Dunaliella tertiolecta*, and *Monoraphidium neglectum*, to nutritional stress have been extensively investigated (González-Ballester et al., 2010; Tan et al., 2016; Jaeger et al., 2017; Lim et al., 2017). The gene expression pattern and regulatory mechanism triggered by N or S depletion for lipid production have been investigated, but without focus on the regulation of starch metabolism (Blaby et al., 2013; Tan et al., 2016; Jaeger et al., 2017; Mao et al., 2020). The omics data reported in the literature confirm that most starch biosynthetic enzymes, such as granule-bound starch synthase, soluble starch synthase, and branching enzyme, were up-regulated with the accumulation of starch under nutrient starvation conditions, and several traditionally recognized starch degradative enzymes, such as starch phosphorylase and amylase, were up-regulated (Ran et al., 2019). The studies conducted using RNA-seq analysis usually obtain a large number of differentially expressed genes (DEGs), and the background is miscellaneous. Thus, starch accumulation in microalgae does not receive much research attention, and the molecular basis for improving starch accumulation and the growth inhibition of nutrient stress, the key factors involved in transcriptional regulation, are largely unclear, especially under sulfur stress conditions.

In this study, *Chlorella sorokiniana*, a fast-growing, thermotolerant, and high-yielding microalgae strain (Lizzul et al., 2018), was investigated to determine whether it could

accumulate a high content of starch under sulfur starvation (SS) conditions. Then, the cells were transferred to sulfur replenishment (SR) conditions to reversely explore the effect of sulfur status on starch accumulation dynamics. Meanwhile, the physiological parameters, namely, cell growth, phenotype, pigment content, and chemical composition, were examined. A time-resolved transcriptome analysis was carried out during the transition of sulfur status, and the sulfur starvation and replenishment cross-validated (SRV)-DEGs were screened to elucidate the underlying mechanisms of starch accumulation and related metabolisms. The potential target genes were identified for the metabolic engineering of *C. sorokiniana* to further improve the capacity of starch production. The expected results could also provide the research basis for process regulation of marine *Chlorella* and related marine biofuel production.

Materials and methods

Strain and culture conditions

C. sorokiniana UTEX1230 was purchased from the Culture Collection of Algae at the University of Texas at Austin (UTEX). The cultivation of *C. sorokiniana* was conducted in 500 mL triangular flasks on a shaker at 25°C, 100 rpm, and with a constant illumination of 80 $\mu\text{mol m}^{-2} \text{s}^{-1}$. The normal growth (NG) condition was maintained in Tris-acetate-phosphate (TAP) medium (Harris, 1989). For sulfur starvation (SS) conditions, the MgSO_4 in the TAP medium was replaced by MgCl_2 at an equal molar concentration. In the second stage, for sulfur replenishment (SR) conditions, 1 mM Na_2SO_4 was added into the SS culture.

Measurement of microalgae growth and pigment content

The cell growth of *C. sorokiniana* was determined by measuring the optical density at 750 nm with a spectrophotometer. The dry biomass yield was calculated based on the dry weight of *C. sorokiniana* and culture volume. For a pigment analysis, fresh samples (2 mL) were centrifuged at 12000 rpm for 3 min, and the pellet was resuspended in 2 mL dimethyl sulfoxide (DMSO). The mixture was then vortexed, and the suspension was centrifuged at 4000 rpm for 5 min to collect the supernatant. The optical densities of the supernatant were measured, and the contents of chlorophyll (chl) A, chl B, and carotenoid were calculated according to a method described in the literature (Wellburn, 1994).

Chemical composition analysis

The carbohydrate content in *C. sorokiniana* was measured according to the protocol of the National Renewable Energy

Laboratory (Wychen and Laurens, 2013). Lyophilized materials weighing 25 mg in dry weight were treated with 72% (w/w) sulfuric acid for 1 h at 30°C in a 15 mL centrifuge tube with a screw cap. The samples were then diluted to 4% sulfuric acid with deionized water and autoclaved for 1 h at 121°C. After cooling, the supernatant was collected for glucose analyses using an SBA 40C bio-sense analyzer (Biology Institute, Shandong Academy of Sciences, China).

The starch content was determined using the enzymic method with thermostable α -amylase and amyloglucosidase (Aladdin, China). Thirty milligrams of lyophilized materials was mixed with 3 mL Na-acetate buffer (pH 5.0), then 0.125 μL α -amylase (2100 u/g) was added, and the solution was heated at 100°C for 60 min. After cooling, 0.125 μL amyloglucosidase (100,000 u/g) was added and heated at 60°C for 60 min. After hydrolysis, the glucose in the supernatant was analyzed using the SBA 40C bio-sense analyzer.

The lipid content was measured using the sulfo-phospho-vanillin (SPV) method (Mishra et al., 2014). The microalgae biomass (3 mg) was suspended in 100 μL water, and 2 mL of concentrated (98%) sulfuric acid was added. The solution was heated for 10 min at 100°C, and it was cooled for 5 min in an ice bath. A total of 5 mL of freshly prepared phospho-vanillin reagent was then added, and the sample was incubated in an incubator shaker for 15 min at 37°C and 200 rpm. The optical density at 530 nm was measured to quantify the lipid content. Corn oil was used to prepare the standard lipid stocks at 50 mg in 50 mL chloroform.

The protein content was measured using a BCA assay kit (Beyotime Institute of Biotechnology, China). Lyophilized microalgal cells were lysed by extraction solution, containing 50 mM Tris (pH 8.1), 1% sodium dodecyl sulfate (SDS), sodium pyrophosphate, β -glycerophosphate, sodium orthovanadate, sodium fluoride, EDTA, and phenylmethanesulfonyl fluoride (PMSF). The supernatant was collected to measure the optical density at 562 nm with the spectrophotometer.

Transmission electron microscopy analysis

The microalgal cells were fixed overnight in 2.5% glutaraldehyde buffer at 4°C. The cells were washed three times with 0.1 M phosphate buffer (pH7.4). The samples were post-fixed in 1% osmic acid at room temperature in the dark for 2 h, and they were dehydrated in gradient ethanol solutions (30%-50%-70%-80%-95%-100%) and in 100% acetone twice at room temperature. After osmotic embedding, polymerization, ultra-thin sectioning, and dyeing, the cellular structure of the cells was observed using a transmission electron microscope (HT7800/HT7700, HITACHI, Japan).

RNA extraction and RNA-seq analysis

Total RNA was extracted using the plant RNA extraction kit (Tiangen Biotech Co., Ltd., Beijing, China). A total of 400 ng RNA per sample was used as input material for the RNA sample preparations. Sequencing libraries were generated using NEBNext[®] UltraTM RNA Library Prep Kit for Illumina[®] (NEB, USA) following the manufacturer's recommendations, and index codes were added to attribute sequences to each sample. The procedure has been described in detail in the literature (Zhang et al., 2021). The clustering of the indexed samples was performed on a cBot Cluster Generation System using TruSeq PE Cluster Kit v3-cBot-HS (Illumina). The RNA sequencing of each sample was conducted using an Illumina Novaseq platform (Novogene Co., Ltd, Tianjin, China), and 150 bp paired-end reads were generated.

Transcriptome *de novo* assembly and differential expression analysis

The data obtained from the sequencing were first spliced into transcripts and subjected to hierarchical clustering using the corset program. RSEM software was used to calculate the gene expression level from the RNA-seq data. R software was used to perform statistics: Pearson correlation between all samples was calculated. Finally, differentially expressed genes (DEGs) between samples were identified, and clustering was carried out using DESeq2 software. The assembled genes were annotated using the BLASTx with an E-value threshold of 1.0 E-5 using the following databases: NCBI non-redundant protein sequences (NR), Clusters of Orthologous Groups of proteins (COG), Swiss-Prot, euKaryotic Ortholog Groups (KOG), Gene Ontology (GO), Protein Family (PFAM), and NCBI nucleotide sequences (NT).

Reverse transcription–polymerase chain reaction analysis

Nine genes were selected for RT-PCR verification. Gene encoding β -actin was used as the internal control. Primers were designed using Primer CE software (Cao et al., 2010). The primers can be found in [Supplementary File 1, Table S1](#). TransZol Up RNA Kit was used to extract the total RNA of *C. sorokiniana*. The cDNA template was obtained using reverse transcription and stored at -20°C for PCR analysis. The PCR reaction system was prepared according to the template, primer structure, and target fragment size in order to obtain the target band. The relative gene expression level was quantified using software Image-Pro Plus 6.0.

Statistical analysis

All experiments were conducted with at least three biological replicates. Experimental results were analyzed using one-way ANOVA with Duncan's multiple range test (SPSS v. 20).

Results

Sulfur status affected cell growth of *C. sorokiniana*

In order to determine the effect of sulfur status on the growth of *C. sorokiniana*, the cultures were observed at different time points under normal growth (NG), sulfur starvation (SS), and sulfur replenishment (SR) conditions by taking photos, and the growth rates and pigment content were investigated (Figure 1). In NG conditions, the culture of *C. sorokiniana* became green as the time increased, but it always maintained a lighter color under SS conditions (Figure 1A). After the transition from SS to SR status, it returned back to its original color within 48 h. The *C. sorokiniana* cells in the TAP medium maintained normal growth (Figures 1B, C). The OD_{750 nm} value reached 3.2, and a 0.9 g/L dry biomass of *C. sorokiniana* was accumulated within 48 h. Under SS conditions, growth was significantly inhibited ($P < 0.01$), and the OD value reached 2.7 within 48 h. As expected, the cell growth and biomass accumulation of *C. sorokiniana* recovered to a certain extent after SR.

The accumulation of chl a, chl b, and carotenoid in *C. sorokiniana* cells increased gradually under NG conditions and decreased substantially under SS conditions ($P < 0.01$). Correspondingly, SR significantly increased the chlorophyll content ($P < 0.01$) (Figures 1D–F). The changes in pigment content during the transition of sulfur status are in accordance with the phenotype alteration.

Sulfur status led to a compositional change in *C. sorokiniana*

Next, the composition of the *C. sorokiniana* biomass, namely, carbohydrates, starch, lipids, and proteins, was analyzed (Figure 2). The carbohydrate content slightly increased within 6 h under NG conditions, and then it remained stable up until 48 h (Figure 2A). By comparison, the carbohydrate content under SS conditions was significantly higher than that under NG conditions after 6 h ($P < 0.01$). It increased from 4.5 to 58.3% of dry weight within 24 h, and then it slightly decreased up until 48 h. Under SR conditions, starting from 24 h, the carbohydrate content significantly decreased within 30 h ($P < 0.01$), and then it returned to the same level as

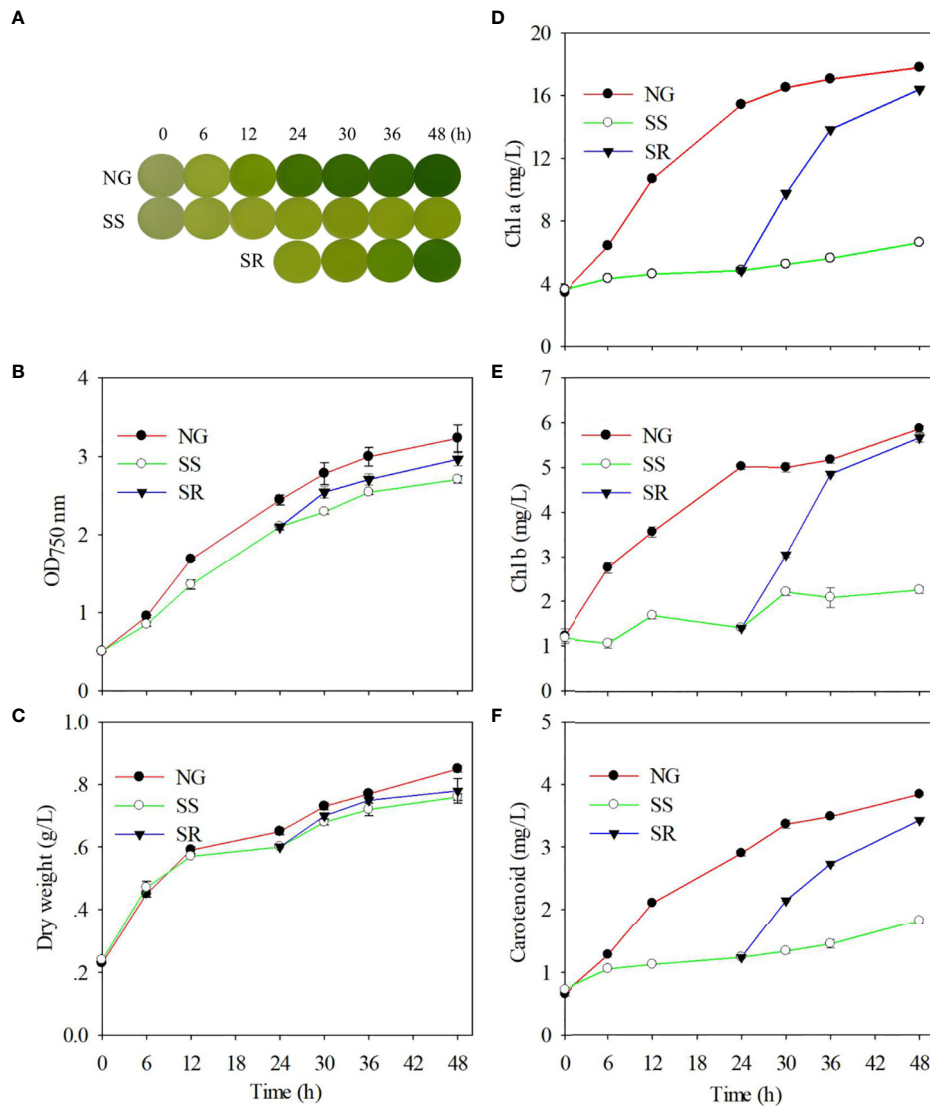


FIGURE 1 Effect of sulfur nutritional status on phenotype (A); optical density during growth (B); dry biomass accumulation (C); and contents of chl a (D), chl b (E), and carotenoid (F) of *C. sorokiniana*. NG, normal growth; SS, sulfur starvation; SR, replenishment.

that under NG conditions by 36 h. The accumulation dynamics of starch were similar to those of carbohydrates (Figure 2B). The maximum starch content of 55.0% was obtained under SS conditions. Starch accounts for approximately 94.3% of the carbohydrate content.

The lipid content also significantly increased from 10.4 to 23.1% within 24 h under SS conditions ($P < 0.01$) and decreased to 11.6% after the SR transition (Figure 2C). The protein content in *C. sorokiniana* under SS conditions significantly decreased from 27.3 to 9.3% within 24 h ($P < 0.01$), and it slightly increased

in up until 48 h. Under SR conditions, after 24 h, the protein content recovered to 36.5%, which is similar to that under NG conditions (Figure 2D).

The cellular morphology of *C. sorokiniana* was examined under each condition via TEM (Figure 3). It was found that *C. sorokiniana* cells became smaller in size under NG conditions, and a pyrenoid formed with a starch granule around it. Under SS conditions, the cell size became larger, the pyrenoid disappeared, and the number of starch granules increased. After the transition to SR, the cellular morphology of *C. sorokiniana* resumed

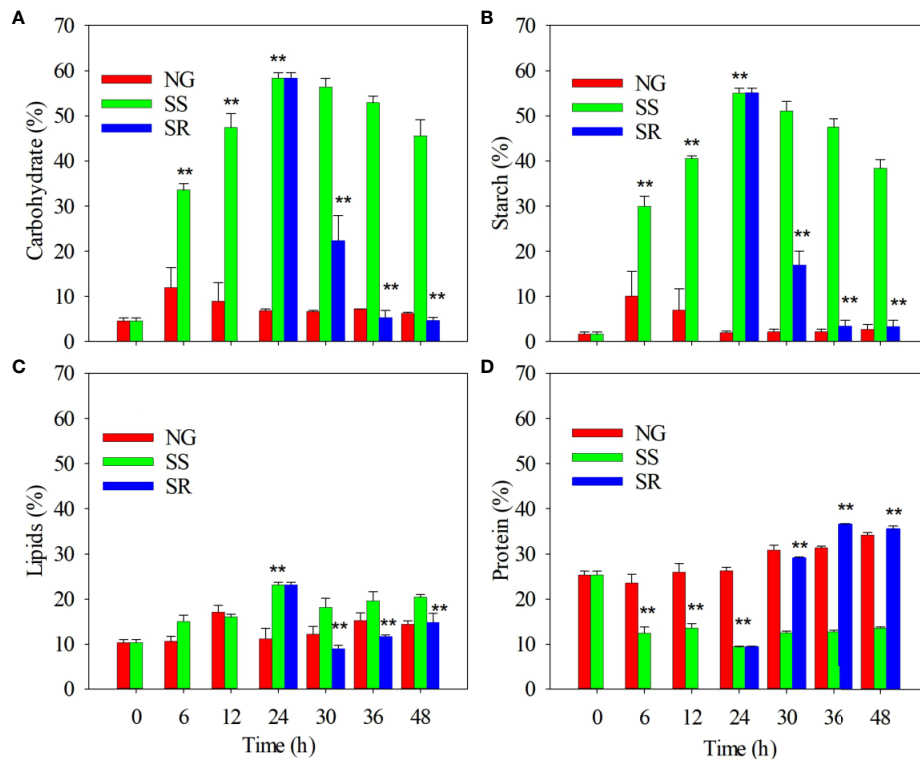


FIGURE 2 Effect of sulfur nutritional status on accumulation of carbohydrates (A), starch (B), lipids (C), and proteins (D) in *C. sorokiniana* cells. NG, normal growth; SS, sulfur starvation; SR, replenishment. The ** indicate the significant differences of samples under SS compared to NG conditions from 6 h to 24 h, and the significant differences of samples under SR compared to SS conditions from 30 h to 48 h.

similarity with that of sample NG-24h. This confirms the enhanced accumulation of starch under SS conditions and the reduction in protein synthesis.

RNA-seq analysis and identification of DEGs

To investigate the molecular basis of enhanced starch accumulation, the transcriptomes of *C. sorokiniana* under NG (0, 6, 12, and 24 h), SS (6, 12, and 24 h), and SR (6, 12, and 24 h) conditions were analyzed using RNA sequencing (Figure 4A).

For each sample, approximately 22.6 million clean reads were obtained and mapped onto the reference genome (Table 1). The transcriptome was assembled *de novo* using trinity, obtaining 61527 transcripts. After assembling the clean reads and eliminating redundancy, 14229 unigenes with an N50 length of 3973 bp were obtained (Supplementary File 2). Subsequently, a final total of 11662 unigenes (81.0%) were annotated in at least one public database, namely, NR, PFAM, GO, Swiss-Prot, NT,

KO, and KOG. In total, 86% of the annotations were obtained by alignment with the publicly available data of *C. sorokiniana*. This high-quality reference transcriptome could be applied in the subsequent analysis of genes' transcriptomic patterns.

According to the Pearson correlation coefficient analysis, the transcription profiles of the 30 samples at ten time points had high repeatability among the three biological replicates (Figure 4B). The changes in transcript abundance relative to sample NG-0h are expressed as log₂FoldChange (FC), and the genes with log₂FC ≥ 1 or ≤ -1 and P_{adj} ≤ 0.05 were regarded as DEGs. As can be seen, a significant transcriptional change was observed between sample NG-0h and SR-6h, followed by SR-12h, NG-12h, SR-24h, SS-12h, NG-24h, SS-6h, and NG-6h. However, global transcriptional cascades were also observed between NG-0h and NG-6h, -12h, and -24h samples because of the growth-induced DEGs. Thus, the background influence should be eliminated. The transcriptional change between the SR-24h and NG-24h samples showed the least difference, which indicated that the cells returned to a normal metabolic stage after transition to SR conditions.

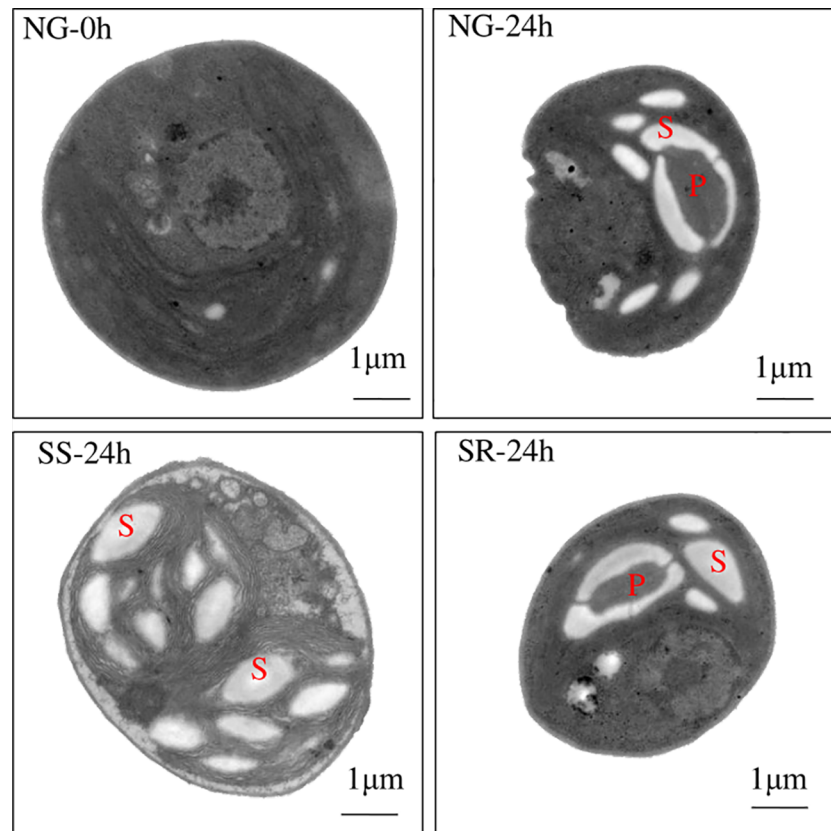


FIGURE 3

Cellular morphology of *C. sorokiniana* under different culture conditions observed using transmission electron microscopy. NG, normal growth; SS, sulfur starvation; SR, replenishment. P, pyrenoid; S, starch granule.

Identification of sulfur starvation and replenishment cross-validated (SRV)-DEGs

A total of 9720 DEGs were identified by comparing pairs, which accounted for 48% of the total unigenes (Figure 5). Compared to the NG-0h sample, there were 2002 up-regulated DEGs and 1137 down-regulated DEGs under NG conditions, and there were 2459 up-regulated DEGs and 1801 down-regulated DEGs under SS conditions. To further identify the DEGs associated with sulfur status, the DEGs co-up-regulated and co-down-regulated in NG and SS conditions were subtracted ($SS \setminus NG$), and, accordingly, 1056 up-regulated and 971 down-regulated DEGs were identified. However, compared to the SS-24h sample, 842 up-regulated and 1039 down-regulated DEGs were observed under SR conditions. Thus, the up-regulated DEGs in the SS treatment, which were simultaneously down-regulated in SR ($\cap SR$), were regarded as sulfur starvation and replenishment cross-validated (SRV)-DEGs. Consequently, 454 SRV-DEGs were identified, among which 283 SRV-DEGs were strongly up-regulated under SS

conditions after from 6 h and down-regulated following the transition to SR after 6 h, and 171 SRV-DEGs showed the opposite expression pattern (Supplementary File 2). This analysis removed the influence of background genes, thus focusing on the important genes that responded to sulfur status.

These SRV-DEGs were then analyzed using the KEGG database (Supplementary File 1, Figure S1). A total of 137 SRV-DEGs were annotated, and 75 SRV-DEGs were enriched to the KEGG metabolic pathways regarding carbohydrates, lipids, amino acids, and energy metabolism; genetic information processing; and signal transduction. It was speculated that these genes were directly correlated with the physiological and biochemical responses of *C. sorokiniana* to sulfur status. However, the SRV-DEGs enriched to the KEGG pathway only accounted for 17% of the total SRV-DEGs, and apparently, many genes were ignored. Thus, the 454 SRV-DEGs were further analyzed based on seven public databases, namely, NR, PFAM, GO, Swiss-Prot, NT, KO, and KOG. The results showed that eight SRV-DEGs were identified in Calvin cycle, seven were identified in starch synthesis pathway, eleven of these

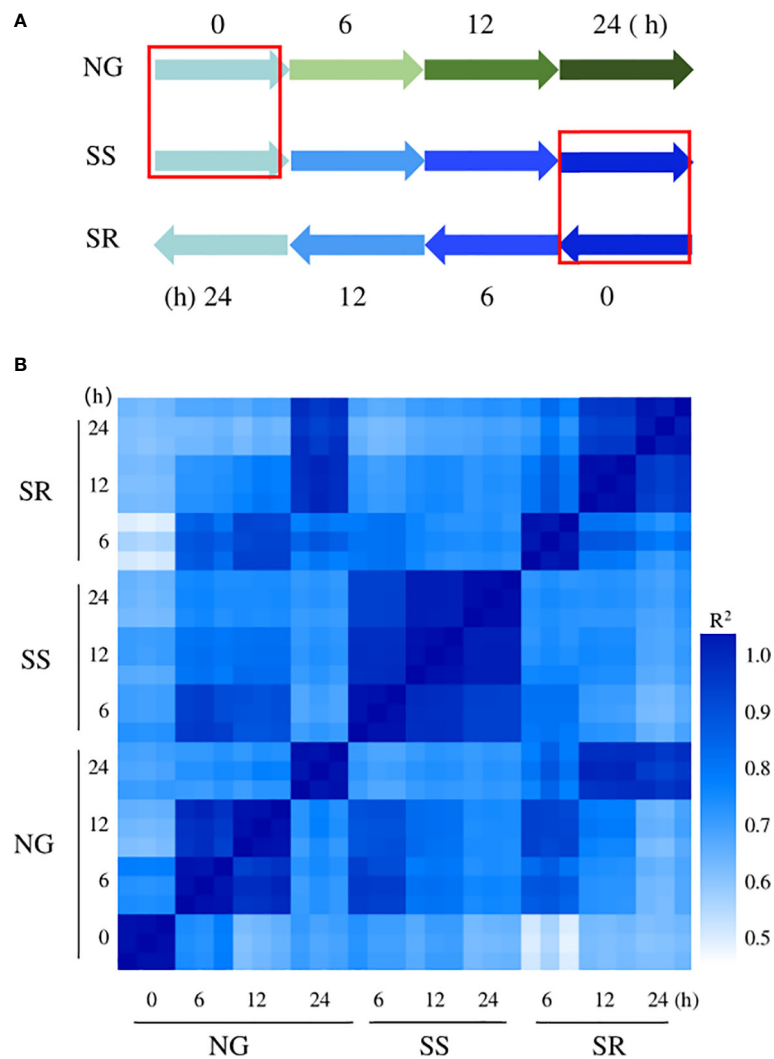


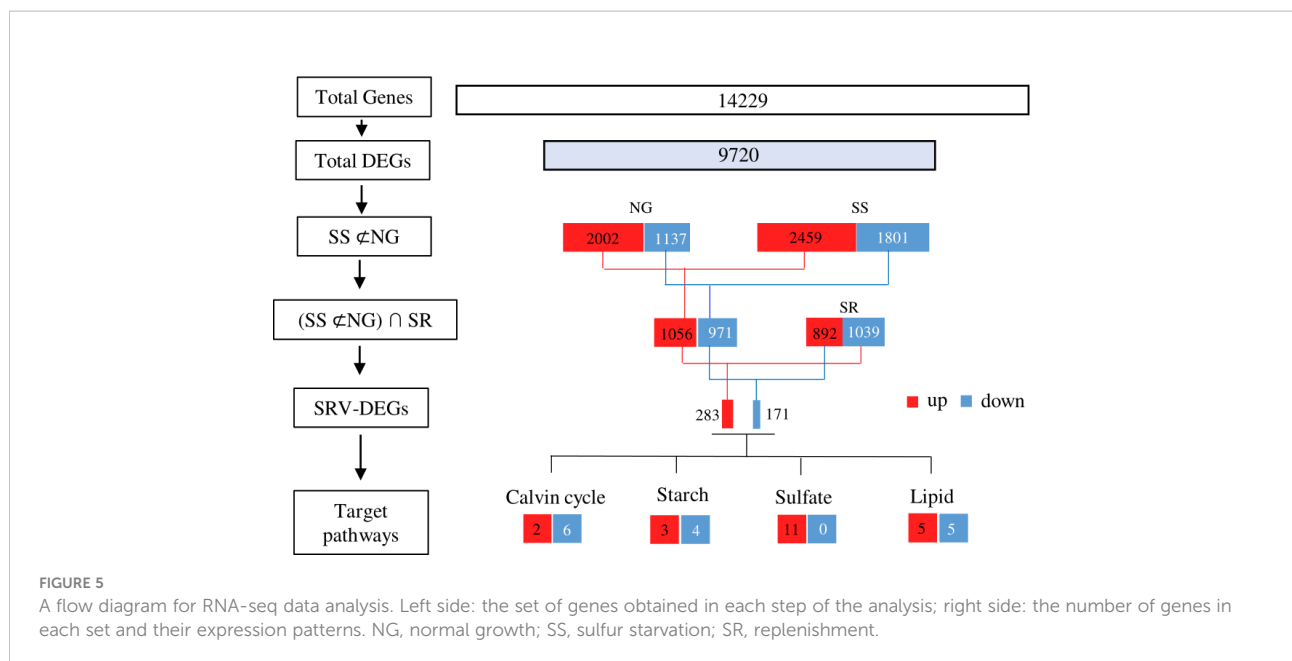
FIGURE 4 Overview of experimental design for RNA-seq analysis. **(A)** Treatments and time points of samples used for RNA-seq analysis, the red frame means the same sample used in the two time points; **(B)** a comparison of all gene expression levels of all samples.

TABLE 1 The *de novo* transcriptome assembly and annotation of *C. sorokiniana*.

Assembly	Results	Annotation	Results
Raw reads	22,683,903	NR	10,405 (73.12%)
Clean reads	22,009,019	PFAM	8,953 (62.92%)
Number of transcripts	61,527	GO	8,953 (62.92%)
Number of unigenes	14,229	Swiss-Prot	6,213 (43.66%)
N50 of transcripts	3,973	NT	5,364 (37.69%)
N50 of genes	3,503	KO	3,710 (26.07%)
		KOG	3,498 (24.58%)
		All annotated	1,086 (7.6%)
		At least one database	11,662 (81%)

were in sulfate metabolism pathway, and ten of these were in lipids synthesis pathway.

Finally, to validate the expression levels of the genes, nine genes were randomly selected for RT-PCR analysis (Supplementary File 1, Figure S2). Basically, the relative expression levels of cysteine synthase[O-acetylserine(thiol)-lyase] (OASTL), fructose-bisphosphate aldolase (FBA), cellulose synthase (CesA), pyruvate kinase (PK), and phosphatidic acid phosphatase (PAP) increased under SS conditions, and decreased after transition from SS to SR conditions. The relative expression levels of RuBP carboxylase/oxygenase (Rubisco), glyceraldehyde 3-phosphate dehydrogenase (GAPDH), and glucose-6-phosphate dehydrogenase (G6PD) decreased under SS conditions, and



increased after transition from SS to SR conditions. According to the results, the expression patterns of most of these genes were consistent with the transcriptome data, indicating the data reliability.

Discussion

SS attenuated photosynthesis

The growth of *C. sorokiniana* is susceptible to sulfur nutritional status. The change in biomass accumulation was consistent with that of cell density, which consequently altered its phenotype. This result is in agreement with that of a previous study of *Chromochloris zofingiensis* subjected to different sulfur nutritional statuses (Mao et al., 2020). SS exerts stress on *C. sorokiniana*, which probably inhibits cellular metabolic processes and the normal development of microalgae, as sulfur is an essential macro-nutrient involved in the synthesis of sulfur-containing proteins and lipids; furthermore, it is related to the synthesis of mercaptan compounds (glutathione), vitamins (thiamine, biotin), thioether and thioester compounds (coenzyme A), polysaccharides, and electron transfer carriers (Lakatos et al., 2019).

The photosynthetic system possibly underwent severe damage during the SS stage, which affected the synthesis of pigments. As previously reported, nutritional changes can cause the oxidative stress of microalgae, which leads to a decline in photosynthetic activity (Chen et al., 2013). The main reason for the decreased level of photosynthesis is the generation of reactive oxygen species (ROS) under nutrient depletion conditions,

which impairs the photosynthetic apparatus (Srinivasan et al., 2018). ROS have been reported to be signaling molecules for metabolic regulations (Mittler et al., 2011). SS can cause an apparent rise in ROS levels, thus leading to a decline in photosynthetic activity (Mao et al., 2020).

In the Calvin cycle (Figure 6), RuBP carboxylase/oxygenase (Rubisco) catalyzes the fixation of CO₂ by incorporating ribulose-1,5-bisphosphate (RuBP), and in this study, its transcript abundance substantially decreased 4.2-fold under SS conditions. Glyceraldehyde 3-phosphate dehydrogenase (GAPDH) catalyzes the conversion of glyceraldehyde-3-phosphate (G3P), which is the common precursor for starch and lipid biosynthesis. G3P is reduced and further converted to fructose-6-phosphate (F6P) by the catalysis of fructose-bisphosphate aldolase (FBA) and fructose 1,6-bisphosphatase (FBPase), and it leaves the Calvin cycle for starch biosynthesis. In this study, the transcriptional levels of GAPDH and FBPase decreased 3.8- and 3.9-fold, respectively. The down-regulated expressions of these enzymes under SS conditions indicate that photosynthesis in the Calvin cycle was reduced, which resulted in the decreased accumulation of pigments (Figures 1D–F). This was probably caused by the oxidative reaction that occurred as the result of sulfur stress (Chen et al., 2017). The decline in photosynthetic activity may be the reason for the inhibition of growth.

SS elevated starch biosynthetic pathway

The starch and protein accumulation in *C. sorokiniana* was susceptible to sulfur nutritional status. The results concerning

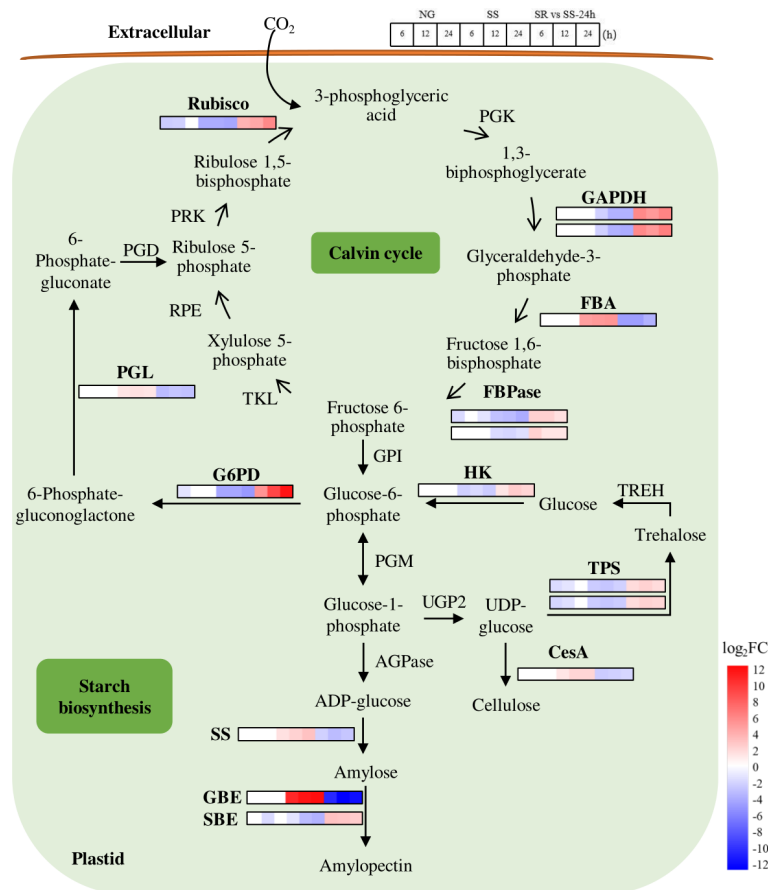


FIGURE 6 Expression patterns of identified SRV-DEGs in starch synthesis pathway of *C. sorokiniana*. Rubisco, RuBP carboxylase/oxygenase; PGK, 3-phosphoglycerate kinase; GAPDH, glyceraldehyde 3-phosphate dehydrogenase; FBA, fructose-bisphosphate aldolase; FBpase, fructose 1,6-bisphosphatase; TKL, transketolase; RPE, ribulose 5-phosphate 3-epimerase; PRK, phosphoribulokinase; G6PD, Glucose-6-phosphate dehydrogenase; PGL, 6-phosphogluconolactonase; PGD, phosphogluconate dehydrogenase; GPI, phosphoglucomutase; PGM, phosphoglucomutase; AGPase, ADP glucose pyrophosphorylase; SS, starch synthase; GBE, glycogen-branching enzyme; SBE, starch branching enzyme; UGP2: UTP-glucose-1-phosphate uridylyltransferase 2; TPS, alpha-trehalose-phosphate synthase; CesaA, cellulose synthase; TREH, alpha-trehalase; HK, Hexokinase. Color legends are shown at the bottom right of the map. The time points of the genes' expression pattern are shown at the top right of the map.

the increased starch accumulation of *C. sorokiniana* under SS conditions are in line with those of previous studies where *Chlorella* and *Parachlorella* were subjected to sulfur limitation conditions (Brányiková et al., 2011; Mizuno et al., 2013; Takeshita et al., 2014; Ota et al., 2016). The sulfur status probably led to changes in cellular metabolic processes, which resulted in redirecting carbon flux from protein biosynthesis toward the synthesis of energy storage metabolites, such as starch. The replenishment of sulfate effectively restored the phenotype and the composition of *C. sorokiniana* within 12 h, which demonstrates the reversible nature of SS-induced metabolic responses.

The starch biosynthesis pathway has been reported in *C. reinhardtii* (Ball, 2002). It starts from the formation of glucose-1-phosphate (Glc-1-P) from Glc-6-P by the catalysis of

phosphoglucomutase (PGM) (Figure 6). Glc-1-P is then converted to ADP-glucose (ADP-Glc) under the catalysis of ADP glucose pyrophosphorylase (AGPase). ADP-Glc serves as the glucose donor for the elongation of the glucan chain to amylose catalyzed by starch synthase (SS). The amylopectin is then formed with the help of repeated branching, elongating, and trimming processes catalyzed by various starch synthetic enzymes, such as glycogen branching enzyme (GBE) and starch branching enzyme (SBE).

In this pathway, the SRV-DEGs encoding SS and GBE were significantly up-regulated 3.0- and 12.0-fold under SS conditions and down-regulated under SR conditions, indicating that these are two key enzymes that contribute to the enhanced formation of amylose and amylopectin and are potential targets for genetic engineering. These results are in agreement with those of a study

that reported that most starch biosynthetic enzymes were up-regulated with the accumulation of starch (Ran et al., 2019). The SRV-DEG encoding SBE showed the opposite expression pattern, indicating the dominant function of GBE in the formation of amylopectin under SS conditions. The traditionally recognized starch degradative enzymes, such as starch phosphorylase (SP) and amylase (AMY), have been reported to be up-regulated under nutrient starvation conditions in most microalgae (Ran et al., 2019). A previous study of *C. sorokiniana* showed that lipid accumulation is largely dependent on starch degradation under N-depleted conditions, and *C. sorokiniana* cells showed the strategy of rerouting the carbon skeleton from starch to lipids (Li et al., 2015). However, in our study, the identified genes encoding starch degradative enzymes were not included in the SRV-DEGs, which was probably due to the early SS stage where lipid was not considerably accumulated. The reason was also possibly because the different mechanism or DEGs caused by N and S limitations.

In addition, trehalose phosphatesynthase (TPS), which catalyzes the formation of trehalose, was down-regulated 3.2-fold under SS conditions. As previously reported, trehalose levels in plants act as protectants against various abiotic stresses (Kosar et al., 2018). Cellulose synthase (CesA) was up-regulated 2.0-fold, indicating changes in the cell wall formation of *C. sorokiniana* under SS conditions. Great transcriptional changes in genes in the oxidative pentose phosphate (OPP) pathway were also observed. Glucose-6-phosphate dehydrogenase (G6PD) decreased 4.9-fold, and 6-phosphogluconolactonase (PGL) increased 1.6-fold under SS conditions, indicating the influence of SS on the starch and lipid biosynthesis pathways. It has been reported that G6PD catalyzes the NADPH-producing steps and that the overexpression of G6PD could elevate NADPH content and, consequently, enhance lipid biosynthesis in microalgae (Xue et al., 2017; Xue et al., 2018).

SS activated sulfur metabolic pathway

Microalgae require sulfur to produce abundant metabolites, such as sulfur-containing amino acids cysteine and methionine, for cell growth and reproduction (Mao et al., 2020). In general, sulfate is transported by SULTR to plastids and is activated by ATP sulfurylase (ATPS) to form 5-adenylyl sulfate (APS) (Leustek et al., 2000) (Figure 7). APS is then converted to 3'-phosphoadenylyl-sulfate (PAPS) and catalyzed by adenylyl sulfate kinase (APK). APS is reduced to sulfide in a two-step reaction catalyzed by APS reductase (APR) and sulfite reductase (SiR). Cysteine is then synthesized from sulfide and O-acetyl-L-serine (OAS) by the catalysis of cysteine synthase [O-acetylserine (thiol)-lyase] (OASTL) and serine acetyltransferase (SAT), and it is then further converted into methionine and glutathione, in which methionine-gamma-lyase (MGL), methionine

aminotransferase (MAT), methanethiol oxidase (SELENBP1), glutathione synthetase (GSS), and glutathione S-transferase (GST) are involved.

In this pathway, the transcriptional abundance of SULTR4 increased 8.6-fold, suggesting the enhanced transportation of sulfate from the cytosol and vacuole to the plastid in *C. sorokiniana* cells by inducing the expression of a high-affinity sulfate transporter (SULTR4). As previously reported, in order to adapt to low-sulfur conditions, the expression of SULTR4 could retrieve the sulfate stored in vacuoles and transfer it to the plastids (Nakashita, 2017). Meanwhile, OASTL and SAT were up-regulated 12.6 and 8.8-fold under SS conditions, respectively, and MGL, MAT, SELENBP1, GSS, and GST were up-regulated 5.9, 2.5, 12.4, 3.4, and 1.8-fold, respectively, which indicate that the cells of *C. sorokiniana* responded distinctly to SS, resulting in intensified formations of cysteine, methionine, and glutathione. These are all likely to be the sensor-like function genes of *C. sorokiniana* used to identify the S status in the growth environment.

Although the expressions of the SRV-DEGs involved in sulfur metabolism were activated under SS conditions, the quantity of the sulfur-containing amino acids was possibly reduced due to the lack of a sulfur source; this is indicated by the results of protein content in *C. sorokiniana* biomass (Figure 2). It is acknowledged that sulfur-containing amino acids are important components for protein synthesis. The inhibition of protein synthesis would increase the accumulation of other amino acids, which can be broken down into α -ketonic acids, such as pyruvate, shifting to the starch and lipid metabolism pathway. However, along with sulfur metabolism, many metabolic pathways, such as photosynthesis and carbon assimilation, are also affected by SS. In this study, these influences consequently resulted in a reduction in production yields, as the growth and biomass accumulation of *C. sorokiniana* both declined.

SS elevated lipid biosynthetic pathway

Lipid is another main storage metabolite in microalgal cells. In order to understand the lipid metabolism of *C. sorokiniana* at the stage of high starch accumulation induced by SS status, the SRV-DEGs encoding the key enzymes in the TAG biosynthesis pathway were identified (Figure 8).

Lipid biosynthesis includes two steps, namely, *de novo* fatty acid synthesis and the subsequent glycerolipid assembly (Ran et al., 2019). In the first step, glyceraldehyde-3-phosphate derived from the Calvin cycle or starch metabolism (degradation) is converted to acetyl-CoA *via* glycolysis (Figure 8). Meanwhile, acetyl-CoA can also be synthesized *via* the conversion of acetate. The results show that the SRV-DEGs encoding pyruvate kinase (PK), which catalyzes the formation of pyruvate, were up-regulated 2.1-fold under SS conditions. The transcript abundance of SRV-DEGs encoding

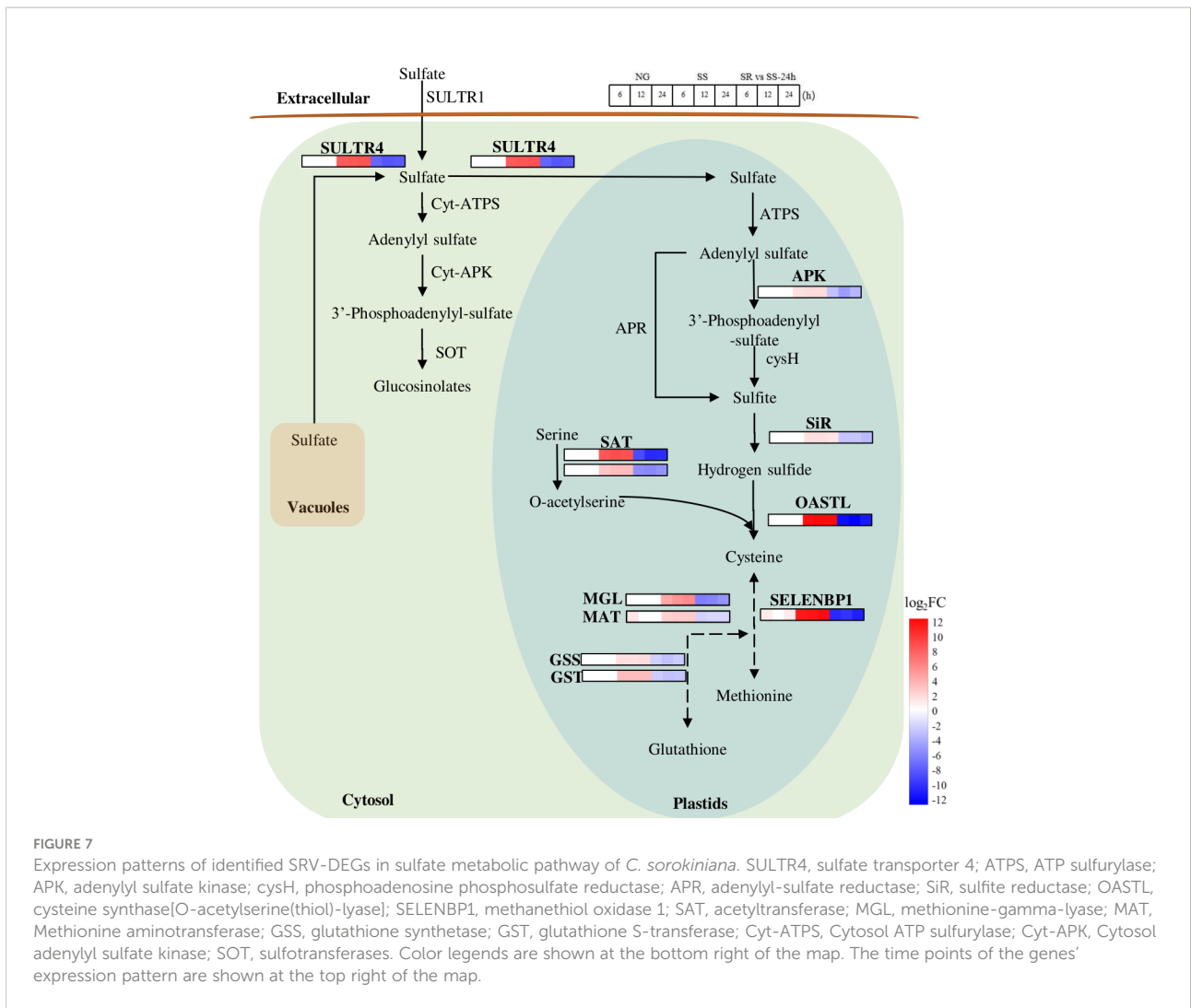


FIGURE 7

Expression patterns of identified SRV-DEGs in sulfate metabolic pathway of *C. sorokiniana*. SULTR4, sulfate transporter 4; ATPS, ATP sulfurylase; APK, adenylyl sulfate kinase; cysH, phosphoadenosine phosphosulfate reductase; APR, adenylyl-sulfate reductase; SiR, sulfite reductase; OASTL, cysteine synthase[O-acetylserine(thiol)-lyase]; SELENBP1, methanethiol oxidase 1; SAT, acetyltransferase; MGL, methionine- γ -lyase; MAT, Methionine aminotransferase; GSS, glutathione synthetase; GST, glutathione S-transferase; Cyt-ATPS, Cytosol ATP sulfurylase; Cyt-APK, Cytosol adenylyl sulfate kinase; SOT, sulfotransferases. Color legends are shown at the bottom right of the map. The time points of the genes' expression pattern are shown at the top right of the map.

aldehyde dehydrogenase (ALDH) and acetyl-CoA synthetase (ACS), which catalyzes the conversion of acetate to acetyl-CoA, decreased -7.0 and -6.7-fold, respectively. The transcriptional change in these genes suggests that the sulfur status affected the metabolic flow of acetyl-CoA, which may have contributed to the increased fatty acid accumulation *via* the glycolysis pathway instead of the conversion from acetate. As previously reported, acetyl-CoA is the precursor for FA synthesis, and the availability of cellular acetyl-CoA plays an important role in TAG accumulation.

In the step of glycerolipid conversion from fatty acids, the SRV-DEGs encoding fatty acid desaturase (FAD), acyl-coenzyme A thioesterase (ACOT), phosphatidic acid phosphatase (PAP), and glycerophosphodiester phosphodiesterase (GDE) were identified. Strong increases in the transcript abundance of FAD (8.9-fold) and PAP (16.2-fold) were observed under SS conditions. However, the generally recognized key genes, such as those encoding glycerol-3-phosphate acyltransferase (GPAT), lysophosphatidate

acyltransferase (LPAT), and diacylglycerol acyltransferase (DGAT), were not identified in these SRV-DEGs. As previously reported, the transcription levels of GPAT and LPAT remained unchanged throughout the SS conditions of *C. zofingiensis*, while the expression of PAP was strongly up-regulated (7.4-fold) (Mao et al., 2020). This suggests that PAP in *C. sorokiniana* is a key rate-limiting enzyme for TAG synthesis.

The results suggest that lipid synthesis was also affected by SS status, although not as many genes were observed to undergo a great change as reported in the literature. The identified genes, such as those encoding FAD, PAP, ACOT, and PK, may have contributed to the enhanced lipid accumulation in *C. sorokiniana* under SS conditions. The accumulation of lipids was lower than that of starch (Figure 2), which was probably due to the preference for starch accumulation of *C. sorokiniana* as the main storage metabolites under stress conditions. The low lipid levels of *C. sorokiniana* could also be because of the early SS stage; as previously reported, *C. sorokiniana* showed a sequential

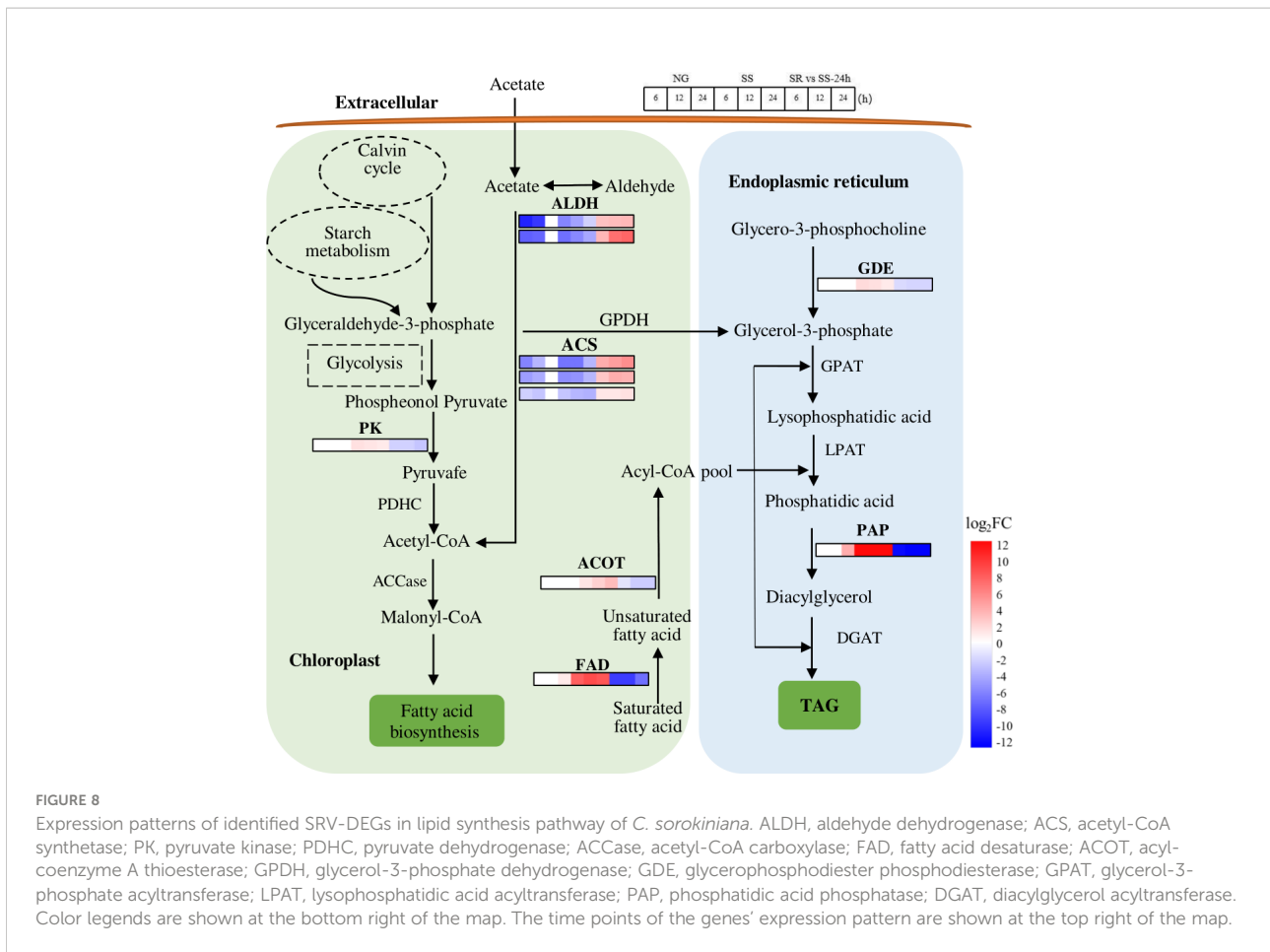


FIGURE 8
 Expression patterns of identified SRV-DEGs in lipid synthesis pathway of *C. sorokiniana*. ALDH, aldehyde dehydrogenase; ACS, acetyl-CoA synthetase; PK, pyruvate kinase; PDHC, pyruvate dehydrogenase; ACCase, acetyl-CoA carboxylase; FAD, fatty acid desaturase; ACOT, acyl-coenzyme A thioesterase; GPDH, glycerol-3-phosphate dehydrogenase; GDE, glycerophosphodiester phosphodiesterase; GPAT, glycerol-3-phosphate acyltransferase; LPAT, lysophosphatidic acid acyltransferase; PAP, phosphatidic acid phosphatase; DGAT, diacylglycerol acyltransferase. Color legends are shown at the bottom right of the map. The time points of the genes' expression pattern are shown at the top right of the map.

accumulation of starch and lipids (Chen et al., 2017). The competitive relationship between starch and lipid synthesis has also been demonstrated in *C. reinhardtii* and *S. obliquus* (Li et al., 2010a; Li et al., 2010b; Jaeger et al., 2014). However, the starch-deficient mutants of *C. sorokiniana* aberrant in isoamylase and starch phosphorylase failed to produce significantly more lipids (Vonlanthen et al., 2015). Thus, there may be more complicated regulatory steps that underlie the partitioning of carbon to these two storage metabolites, and this study provided potential target genes that could be applied in genetic engineering to investigate the relationship between starch and lipid accumulation in *C. sorokiniana*, guiding the process regulation for biofuels production.

Conclusion

C. sorokiniana accumulated a considerable amount of starch rather than lipids under SS conditions. For the molecular basis

investigation, this study developed a strategy to identify the key SRV-DEGs associated with sulfur responses by cross-validation under SS and SR conditions. In total, 454 SRV-DEGs were identified, which accounted for 4.7% of the total DEGs. The sensor-like SRV-DEGs, such as those encoding SULTR, SAT, OASTL, and SELENBP, in the sulfate metabolic pathway were first identified in the SS environment, and then they resulted in the reallocation of carbon and elevated the starch synthesis pathway. The SRV-DEGs encoding GBE and starch synthase (SS) in the starch synthesis pathway serve as the key genes regulating starch accumulation in *C. sorokiniana*. However, cell growth was inhibited, possibly because of the down-regulation of the genes associated with carbon fixation. An in-depth study of these SRV-DEGs in related metabolic pathways revealed the underlying starch accumulation mechanism, as well as the relationship with cell growth and lipid synthesis. These genes may be potential target genes that could be applied in metabolic engineering to further improve the starch production capacity of *C. sorokiniana*.

Data availability statement

The original contributions presented in the study are included in the article/Supplementary Material. Further inquiries can be directed to the corresponding authors. The sequencing data presented in the study are deposited in the NCBI Bioproject repository, accession number PRJNA814463.

Author contributions

HX: Experiment conduction, data analysis, figures production. JY, XW, QP, YH, XL and KL: Methodology, formal analysis. SD and LL: Review and editing. GL: Conceptualization, supervision, review and editing. MY: Conceptualization, supervision, writing – original draft, writing – review & editing. All authors contributed to the article and approved the submitted version.

Funding

This work was supported by the Hebei Natural Science Foundation (B2021204034), the Key Research and Development Program in Hebei Province (21322917D), the Fundamental Research Funds for the Provincial Universities of

Hebei (KY2021040), and the Start-up Fund for Introduced Talents of Hebei Agricultural University (YJ201910).

Conflict of interest

The authors declare that the research was conducted in the absence of any commercial or financial relationships that could be construed as a potential conflict of interest.

Publisher's note

All claims expressed in this article are solely those of the authors and do not necessarily represent those of their affiliated organizations, or those of the publisher, the editors and the reviewers. Any product that may be evaluated in this article, or claim that may be made by its manufacturer, is not guaranteed or endorsed by the publisher.

Supplementary material

The Supplementary Material for this article can be found online at: <https://www.frontiersin.org/articles/10.3389/fmars.2022.986400/full#supplementary-material>

References

- Ball, S. G. (2002). The intricate pathway of starch biosynthesis and degradation in the monocellular alga *Chlamydomonas reinhardtii*. *Aust. J. Chem.* 55, 45–59. doi: 10.1071/CH02052
- Blaby, I. K., Glaesener, A. G., Mettler, T., Fitz-Gibbon, S. T., Gallaher, S. D., Liu, B., et al. (2013). Systems-level analysis of nitrogen starvation-induced modifications of carbon metabolism in a *Chlamydomonas reinhardtii* starchless mutant. *Plant Cell*. 25, 4305–4323. doi: 10.1105/tpc.113.117580
- Brányiková, I., Marálková, B., Doucha, J., Brányik, T., Bišová, K., Zachleder, V., et al. (2011). Microalgae-novel highly efficient starch producers. *Biotechnol. Bioeng.* 108, 766–776. doi: 10.1002/bit.23016
- Cao, Y. H., Sun, J., Zhu, J. H., Li, L. Y., and Liu, G. Z. (2010). PrimerCE: designing primers for cloning and gene expression. *Mol. Biotechnol.* 46, 113–117. doi: 10.1007/s12033-010-9276-3
- Chen, B. L., Wan, C., Mehmood, M. A., Chang, J. S., Bai, F. W., and Zhao, X. Q. (2017). Manipulating environmental stresses and stress tolerance of microalgae for enhanced production of lipids and value-added products—a review. *Bioresour. Technol.* 244, 1198–2206. doi: 10.1016/j.biortech.2017.05.170
- Chen, C. Y., Zhao, X. Q., Yen, H. W., Ho, S. H., Cheng, C. L., Lee, D. J., et al. (2013). Microalgae-based carbohydrates for biofuel production. *Biochem. Eng. J.* 78, 1–10. doi: 10.1016/j.bej.2013.03.006
- Demuez, M., Mahdy, A., Tomas-Pejo, E., Gonzalez-Fernandez, C., and Ballesteros, M. (2015). Enzymatic cell disruption of microalgae biomass in biorefinery processes. *Biotechnol. Bioeng.* 112, 1955–1966. doi: 10.1002/bit.25644
- Fernandes, B., Teixeira, J., Dragone, G., Vicente, A. A., Kawano, S., Bišová, K., et al. (2013). Relationship between starch and lipid accumulation induced by nutrient depletion and replenishment in the microalga *Parachlorella kessleri*. *Bioresour. Technol.* 144, 268–274. doi: 10.1016/j.biortech.2013.06.096
- Gardner, R. D., Lohman, E., Gerlach, R., Cooksey, K. E., and Peyton, B. M. (2012). Comparison of CO₂ and bicarbonate as inorganic carbon sources for triacylglycerol and starch accumulation in *Chlamydomonas reinhardtii*. *Biotechnol. Bioeng.* 110, 87–96. doi: 10.1002/bit.24592
- González-Ballester, D., Casero, D., Cokus, S., Pellegrini, M., Merchant, S. S., and Grossman, A. R. (2010). RNA-Seq analysis of sulfur-deprived *Chlamydomonas* cells reveals aspects of acclimation critical for cell survival. *Plant Cell*. 22, 2058–2084. doi: 10.1105/tpc.109.071167
- Harris, E. H. (1989). *The Chlamydomonas sourcebook: A comprehensive guide to biology and laboratory use* (San Diego, CA: Academic Press).
- Jaeger, L., Verbeek, R. E., Draaisma, R. B., Martens, D. E., Springer, J., Eggink, G., et al. (2014). Superior triacylglycerol (TAG) accumulation in starchless mutants of *Scenedesmus obliquus*: (I) mutant generation and characterization. *Biotechnol. Biofuels*. 1, 69. doi: 10.1186/1754-6834-7-69
- Jaeger, D., Winkler, A., Mussgnug, J. H., Kalinowski, J., Goesmann, A., and Kruse, O. (2017). Time-resolved transcriptome analysis and lipid pathway reconstruction of the oleaginous green microalga *Monoraphidium neglectum* reveal a model for triacylglycerol and lipid hyperaccumulation. *Biotechnol. Biofuels*. 10, 197. doi: 10.1186/s13068-017-0882-1
- Kosar, F., Akram, N. A., Sadiq, M., Qurainy, F. A., and Ashraf, M. (2018). Trehalose: A key organic osmolyte effectively involved in plant abiotic stress tolerance. *J. Plant Growth Regul.* 38, 606–618. doi: 10.1007/s00344-018-9876-x
- Lakatos, G. E., Ranglová, K., Manoel, J. C., Grivalský, T., Kopecký, J., and Masojidek, J. (2019). Bioethanol production from microalgae polysaccharides. *Folia Microbiol.* 64, 627–644. doi: 10.1007/s12223-019-00732-0
- Leustek, T., Martin, M. N., Bick, J. A., and Davies, J. P. (2000). Pathways and regulation of sulfur metabolism revealed through molecular and genetic studies. *Annu. Rev. Plant Physiol. Plant Mol. Biol.* 51, 141–165. doi: 10.1146/annurev.arplant.51.1.141
- Li, T. T., Gargouri, M., Feng, J., Park, J. J., Gao, D. F., Miao, C., et al. (2015). Regulation of starch and lipid accumulation in a microalga *Chlorella sorokiniana*. *Bioresour. Technol.* 180, 250–257. doi: 10.1016/j.biortech.2015.01.005

- Li, Y. T., Han, D. X., Hu, G. R., Dauvillee, D., Sommerfeld, M., Ball, S., et al. (2010a). *Chlamydomonas* starchless mutant defective in ADP-glucose pyrophosphorylase hyper-accumulates triacylglycerol. *Metab. Eng.* 12, 387–391. doi: 10.1016/j.ymben.2010.02.002
- Li, Y. T., Han, D. X., Hu, G. R., Sommerfeld, M., and Hu, Q. (2010b). Inhibition of starch synthesis results in overproduction of lipids in *Chlamydomonas reinhardtii*. *Biotechnol. Bioeng.* 107, 258–268. doi: 10.1002/bit.22807
- Lim, D. K. Y., Schuhmann, H., Hall, S. R. T., Chan, K. C. K., Wass, T. J., Aguilerab, F., et al. (2017). RNA-Seq and metabolic flux analysis of *Tetraselmis* sp. M8 during nitrogen starvation reveals a two-stage lipid accumulation mechanism. *Bioresour. Technol.* 244, 1281–1293. doi: 10.1016/j.biortech.2017.06.003
- Lizzul, A. M., Lekuona-Amundarain, A., Purton, S., and Campos, L. C. (2018). Characterization of *Chlorella sorokiniana*, UTEX 1230. *Biology* 7, 25. doi: 10.3390/biology7020025
- Mao, X. M., Lao, Y. M., Sun, H., Li, X. J., Yu, J. F., and Chen, F. (2020). Time resolved transcriptome analysis during transitions of sulfur nutritional status provides insight into triacylglycerol (TAG) and astaxanthin accumulation in the green alga *Chromochloris zofingiensis*. *Biotechnol. Biofuels.* 13, 128. doi: 10.1186/s13068-020-01768-y
- Mishra, S. K., Suh, W. I., Farooq, W., Moon, M., Shrivastav, A., Park, M. S., et al. (2014). Rapid quantification of microalgal lipids in aqueous medium by a simple colorimetric method. *Bioresour. Technol.* 155, 330–333. doi: 10.1016/j.biortech.2013.12.077
- Mittler, R., Vanderauwera, S., Suzuki, N., Miller, G., Tognetti, V. B., Vandepoele, K., et al. (2011). ROS signaling: the new wave? *Trends Plant Sci.* 16, 300–309. doi: 10.1016/j.tplants.2011.03.007
- Mizuno, Y., Sato, A., Watanabe, K., Hirata, A., Takeshita, T., Ota, S., et al. (2013). Sequential accumulation of starch and lipid induced by sulfur deficiency in *Chlorella* and *Parachlorella* species. *Bioresour. Technol.* 129, 150–155. doi: 10.1016/j.biortech.2012.11.030
- Nakashita, A. M. (2017). Metabolic changes sustain the plant life in low-sulfur environments. *Curr. Opin. Plant Biol.* 39, 144–151. doi: 10.1016/j.pbi.2017.06.015
- Ota, S., Oshima, K., Yamazaki, T., Kim, S., Yu, Z., Yoshihara, M., et al. (2016). Highly efficient lipid production in the green alga *Parachlorella kessleri*: Draft genome and transcriptome endorsed by whole-cell 3D ultrastructure. *Biotechnol. Biofuels.* 9, 13. doi: 10.1186/s13068-016-0424-2
- Ran, W. Y., Wang, H. T., Liu, Y. H., Qi, M., Xiang, Q., Yao, C. H., et al. (2019). Storage of starch and lipids in microalgae: Biosynthesis and manipulation by nutrients. *Bioresour. Technol.* 291, 121894. doi: 10.1016/j.biortech.2019.121894
- Srinivasan, R., Mageswari, A., Subramanian, P., Suganthi, C., Chaitanyakumar, A., Aswini, V., et al. (2018). Bicarbonate supplementation enhances growth and biochemical composition of *Dunaliella salina* V-101 by reducing oxidative stress induced during macronutrient deficit conditions. *Sci. Rep.* 8, 6972. doi: 10.1038/s41598-018-25417-5
- Su, Y. J., Song, K. H., Zhang, P. D., Su, Y. Q., Cheng, J., and Chen, X. (2017). Progress of microalgae biofuel's commercialization. *Renew. Sust. Energ. Rev.* 74, 402–411. doi: 10.1016/j.rser.2016.12.078
- Takeshita, T., Ota, S., Yamazaki, T., Hirata, A., Zachleder, V., and Kawano, S. (2014). Starch and lipid accumulation in eight strains of six *Chlorella* species under comparatively high light intensity and aeration culture conditions. *Bioresour. Technol.* 158, 127–134. doi: 10.1016/j.biortech.2014.01.135
- Tan, K. W. M., Lin, H., Shen, H., and Lee, Y. K. (2016). Nitrogen-induced metabolic changes and molecular determinants of carbon allocation in *Dunaliella tertiolecta*. *Sci. Rep.* 6, 37235. doi: 10.1038/srep37235
- Vonlanthen, S., Dauvillee, D., and Purton, S. (2015). Evaluation of novel starch-deficient mutants of *Chlorella sorokiniana* for hyper-accumulation of lipids. *Algal Res.* 12, 109–118. doi: 10.1016/j.algal.2015.08.008
- Wang, Y., Ho, S. H., Yen, H. W., Nagarajan, D., Ren, N. Q., Li, S. F., et al. (2017). Current advances on fermentative biobutanol production using third generation feedstock. *Biotechnol. Adv.* 35, 1049–1059. doi: 10.1016/j.biotechadv.2017.06.001
- Wellburn, A. R. (1994). The spectral determination of chlorophylls a and b, as well as total carotenoids, using various solvents with spectrophotometers of different resolution. *J. Plant Physiol.* 144, 307–313. doi: 10.1016/S0176-1617(11)81192-2
- Wyche, S. V., and Laurens, L. M. L. (2013). *Determination of total carbohydrates in algal biomass*. (Golden, CO, United States: National Renewable Energy Lab. (NREL)).
- Xue, J., Balamurugan, S., Li, D. W., Liu, Y. H., Zeng, H., Wang, L., et al. (2017). Glucose-6-phosphate dehydrogenase as a target for highly efficient fatty acid biosynthesis in microalgae by enhancing NADPH supply. *Metab. Eng.* 41, 212–221. doi: 10.1186/s12934-019-1214-x
- Xue, J., Chen, T. T., Zheng, J. W., Balamurugan, S., Cai, J. X., Liu, Y. H., et al. (2018). The role of diatom glucose-6-phosphate dehydrogenase on lipogenic NADPH supply in green microalgae through plastidial oxidative pentose phosphate pathway. *Appl. Microbiol. Biot.* 102, 10803–10815. doi: 10.1007/s00253-018-9415-5
- Yao, C. H., Ai, J. N., Cao, X. P., Xue, S., and Zhang, W. (2012). Enhancing starch production of a marine green microalga *Tetraselmis subcordiformis* through nutrient limitation. *Bioresour. Technol.* 118, 438–444. doi: 10.1016/j.biortech.2012.05.030
- Yao, C. H., Jiang, J. P., Cao, X. P., Liu, Y. H., Xue, S., and Zhang, Y. K. (2018). Phosphorus enhances photosynthetic storage starch production in a green microalga (Chlorophyta) *Tetraselmis subcordiformis* in nitrogen starvation conditions. *J. Agr. Food Chem.* 66, 10777–10787. doi: 10.1021/acs.jafc.8b04798
- Zhang, Y. F., Gu, Z. P., Ren, Y. D., Wang, L., Zhang, J., Liang, C. W., et al. (2021). Integrating transcriptomics and metabolomics to characterize metabolic regulation to elevated CO₂ in *Chlamydomonas reinhardtii*. *Mar. Biotechnol.* 23, 255–275. doi: 10.1007/s10126-021-10021-y